

## Supplementary Methods

### *Animal experimental design*

The glomerular basement membrane (GBM)-reactive rabbit anti-mouse glomerular lysate nephrotoxic serum (NTS) was produced by Lampire Laboratories as elaborated elsewhere.<sup>1</sup> Male wild-type (WT) and e/e mice aged 10 weeks old received intraperitoneal injection of 250 $\mu$ l rabbit IgG emulsified in complete Freund's adjuvant (Santa Cruz Biotechnology) 6 days before tail vein injection of NTS at a dose of 10  $\mu$ l/g body *wt* to induce nephritis. As controls, mice received injection of equal volumes of nonimmune IgG. Three days after NTS injection, mice with inadequate glomerular injury, as indicated by less than 2+ on urine protein dipstick tests, were excluded. Mice were then randomized to receive daily subcutaneous (s.c.) injections of an equal dose (0.7 $\mu$ mol/kg/d) of NDP-MSH or MS05 (custom peptide service, GL Biochem) or vehicle, or every other day treatment with s.c. injection of the Repository Corticotropin Injection (RCI) (Acthar® Gel, 60IU/kg/q.o.d., Mallinckrodt ARD) or an equal volume of vehicle gelatin gel. Severely sick mice were humanely culled. The doses of synthetic melanocortins and RCI were adopted based on previous studies<sup>2, 3</sup> and verified by pilot experiments. Mice were euthanized on day 1 or 14 after NTS injury, and blood, urine, spleen and kidney specimens were collected for further examination.

### *Urine and serum analyses*

Urine albumin concentration was measured by using a mouse albumin enzyme-linked immunosorbent assay (ELISA) quantitation kit (Bethyl Laboratories Inc.). Urine creatinine concentration was measured by a creatinine assay kit (BioAssay Systems). Blood urea nitrogen (BUN) in sera was measured by using a commercial urea assay kit (BioAssay Systems) according to the manufacturer's instruction.

### *Kidney histology*

Formalin-fixed paraffin-embedded kidney specimens were prepared in 3- $\mu$ m-thick sections and subjected to periodic acid-Schiff (PAS) staining. A semi-quantitative glomerulonephritis (GN) score was used to evaluate the degree of glomerular injury, featured by glomerular hypercellularity, crescent formation, mesangial expansion, inflammation and fibrosis. The morphologic features of all sections were assessed by a single observer in a blinded manner. The severity of glomerulonephritis was graded from 0 to 4 as follows: 0, normal; 1, mild increase in glomerular cellularity and mesangial matrix; 2, moderate increase in glomerular cellularity and mesangial matrix with thickening of the GBM; 3, focal endocapillary hypercellularity with obliteration of capillary lumen and a substantial increase in the thickness and irregularity of the GBM; and 4, diffuse endocapillary hypercellularity, segmental necrosis, crescents, and hyalinized sclerotic glomeruli. Likewise, the severity of tubulointerstitial nephritis (TIN) was scored from 0-4 scale on the basis of severity of tubular atrophy, dilatation and interstitial inflammation and fibrosis.<sup>4</sup> The percentage of glomeruli with crescent formation was estimated by absolute counting and expressed as a percentage of 30 random glomeruli per mouse kidney specimen.

### *Isolation of glomeruli*

Following mouse euthanasia and resection of left kidneys, right kidneys were perfused with phosphate buffered saline (PBS) containing Dynabeads M-450 (DynaL Biotech ASA) or magnetic iron oxide particles (Sigma-Aldrich). Kidney cortices were minced into 1-mm<sup>3</sup> pieces and digested in collagenase A (1 mg/ml, Sigma-Aldrich). After the digested tissue was gently pressed through a 100- $\mu$ m cell strainer (BD Falcon), glomeruli were

collected and then purified using a magnetic particle concentrator. An aliquot of isolated glomeruli was examined under a microscope to ensure that samples contained fewer than 5 tubules per  $\times 200$  field.

#### *Culture of bone marrow-derived macrophages*

Bone marrow-derived cells (BMDCs) prepared from WT or *e/e* mice were cultured with RPMI 1640 medium containing 10% fetal bovine serum (FBS) and granulocyte-macrophage colony-stimulating factor (GM-CSF; 10ng/ml; R&D Systems, Inc.) for 7 days. Then the adherent cells were harvested and characterized to be bone marrow-derived macrophages (BMM). BMM cells were primed with a mix of LPS (100ng/ml; Sigma-Aldrich) and IFN- $\gamma$  (50ng/ml; Cell Signaling Technology) for 4 days for M1 polarization in the presence or absence of MS05 ( $10^{-7}$ M) or pyrrolidine dithiocarbamate (PDTC, 2.5 $\mu$ M, Sigma-Aldrich). Cells were then collected and examined.

#### *In vitro immune response of splenocyte cultures*

After euthanasia, spleens were removed from WT or *e/e* mice 2 weeks after NTS injury and were dissociated into single cell suspensions by using a 70- $\mu$ m cell strainer. To obtain the purified splenocytes, single cell suspensions were subjected to red blood cell lysis with the red blood cell lysis buffer containing 154 mM NH<sub>4</sub>Cl, 10 mM KHCO<sub>3</sub>, and 100  $\mu$ M Na<sub>2</sub> EDTA. Splenocytes were then cultured in RPMI medium supplemented with 10% FBS, 2 mM L-glutamine, 100 U/mL penicillin, 100  $\mu$ g/mL streptomycin, 1 mM sodium pyruvate, 1 mM non-essential amino acids and 50  $\mu$ M 2-mercaptoethanol, and stimulated with rabbit IgG (50  $\mu$ g/mL) in the presence or absence of MS05 ( $10^{-7}$ M) or PDTC (2.5 $\mu$ M). After 6 days, the supernatants and cells were separated and processed for further examination. Alternatively, the freshly purified splenocytes were stained with anti-CD3 (Biolegend) and anti-CD19 antibodies (Biolegend), and T and B lymphocytes were respectively isolated by fluorescence-activated cell sorting and processed for immunoblot analysis.

#### *Immunofluorescence staining*

Cryosections of kidneys were fixed with 4% paraformaldehyde (Sigma-Aldrich), permeabilized, and stained with Alexa Fluor-conjugated antibodies against synaptopodin (Santa Cruz Biotechnology), C5b-9 (Santa Cruz Biotechnology), FITC anti-mouse F4/80 (Biolegend), Alexa Fluor 594 anti-inducible nitric oxide synthase (iNOS) (Biolegend), Alexa Fluor 647 anti-mouse mannose receptor (MR) (Biolegend) antibodies. Alternatively, kidney frozen sections were incubated with primary antibodies against podocin (Santa Cruz Biotechnology), desmin (Santa Cruz Biotechnology), WT-1 (Santa Cruz Biotechnology), mouse IgG1 (Biolegend), mouse IgG2c (encoded by immunoglobulin heavy chain 1b or *Igh-1b* allele) (Jackson ImmunoResearch), mouse IgG3 (Biolegend) or forkhead box protein P3 (FoxP3) (Santa Cruz Biotechnology), followed by staining with Alexa Fluor-conjugated secondary antibodies (Life Technologies). Finally, sections were mounted with Vectashield mounting medium with or without 4',6-diamidino-2-phenylindole (DAPI) (Vector Laboratories). As negative controls, the primary antibodies were replaced by IgG isotype controls from the same species of the primary antibodies and no specific staining was noted (Supplementary Figure S10). To evaluate glomerular deposition of heterologous or autologous IgG, frozen sections were stained with Alexa Fluor-conjugated anti-rabbit or anti-mouse IgG (Life Technologies). As negative controls, Alexa Fluor-conjugated anti-goat IgG was applied and no specific staining was detected (Supplementary Figure S10). Fluorescence staining was visualized using a fluorescence microscope (EVOS FL, Thermo Fisher Scientific) or a Leica TCS SP5 multiphoton laser scanning confocal microscope (Leica Microsystems Inc.).

#### *Kidney leukocyte isolation*

Kidney leukocytes were isolated from mice with NTS nephritis as reported before.<sup>5</sup> In brief, after mice were euthanized, kidneys were perfused and collected. Renal tissues were finely minced and digested for 30 minutes at 37°C with 1 mg/ml collagenase (Sigma-Aldrich) and 0.01 mg/ml DNase. Tissue suspensions were sequentially passed through 70 and 40 µm strainers and rinsed with Hank's balanced salt solution (Sigma-Aldrich). Mononuclear leukocytes were isolated by centrifugation in a Percoll gradient. Cells were washed and resuspended for further examination.

#### *Flow cytometry analyses*

Kidney leukocytes were stained with fluorochrome-conjugated antibodies against CD3 (Biolegend), CD19 (Biolegend) and F4/80 (Biolegend). Alternatively, cells were incubated with antibodies against CD45 (Genetex) or MC1R (Santa Cruz Biotechnology) followed by staining with FITC or Alexa Fluor 647-conjugated secondary antibodies. Cells were subsequently rinsed and resuspended in wash buffer. Flow cytometry was then carried out with a flow cytometer (BD Biosciences) and data analyzed with FlowJo Software.

#### *Assay of signature cytokines of Th immunity*

Expression levels of T lymphocyte-related cytokines (IL2, IL4, IL6, IL10, IFN-γ and TNF-α) in kidneys derived from NTS-injured vehicle-treated WT or e/e mice were simultaneously analyzed using the mouse Cytometric Bead Array kit (BD Biosciences) according to the manufacturer's instruction. In essence, 50 µL of kidney homogenates or standard cytokines was incubated with 50 µL of bead mixture and phycoerythrin (PE)-conjugated detection antibodies at room temperature. After 2 hours, beads were rinsed with 1 mL of wash buffer, and samples were subsequently analyzed on a dual-laser flow cytometer. FlowJo software was used to measure median fluorescence intensity of each cytokine, and cytokine concentrations were calculated according to standard curves prepared simultaneously.

#### *ELISA of rabbit IgG-specific mouse IgG levels*

ELISA microplates coated with 10 µg/ml of rabbit IgG (Jackson ImmunoResearch) were incubated with serum samples diluted at 1:200~ 1:20,000 or conditioned medium after blocking with 1% bovine serum albumin. After washing with PBS containing 0.05% Tween 20, the plates were incubated with horseradish peroxidase (HRP)-conjugated goat anti-mouse IgG (Invitrogen), or with rat anti-mouse IgG1, IgG3 antibodies (Biolegend) or goat anti-mouse IgG2c antibody (Jackson ImmunoResearch) followed by detection with HRP-conjugated chicken anti-rat (Abcam) or donkey anti-goat IgG (Invitrogen). For color development, 3,3',5,5'-tetramethylbenzidine was used. The reaction was terminated by adding 100 µl per well of 1 M sulfuric acid, and absorbance was measured at 450 nm using a microplate spectrophotometer (Cytation 5, BioTek Instruments).

#### *Bioinformatics analysis of publicly-available transcriptomic data*

Single cell RNA sequencing (scRNAseq) transcriptomic data of kidney biopsies from lupus patients are publicly available and collected at the Single Cell Portal ([https://singlecell.broadinstitute.org/single\\_cell/study/SCP279/amp-phase-1](https://singlecell.broadinstitute.org/single_cell/study/SCP279/amp-phase-1)) based on data derived from the Accelerating Medicines Partnership (AMP) Phase I Studies of Lupus Nephritis.<sup>6</sup> The mRNA expression levels of various MCR in diverse renal leukocytes were analyzed. In addition, the transcriptomic data of peripheral blood mononuclear cells (PBMC) derived from patients with systemic lupus erythematosus (SLE) are publicly available (GEO accession number: GSE121239).<sup>7</sup> The associations between MC1R expression and curated gene sets involved in immune regulatory pathways were examined by gene set enrichment analysis (GSEA), which was performed by employing GSEA v4.2.3 software

(<http://software.broadinstitute.org/gsea/index.jsp>).

### *Western immunoblot analysis*

Kidney specimens, isolated kidney glomeruli or cultured or isolated cells were lysed in radioimmunoprecipitation assay buffer supplemented with protease inhibitors, and samples were processed for immunoblot analysis as previously elaborated.<sup>8</sup> The primary antibodies against podocin, WT-1, IL-1 $\beta$ , actin and glyceraldehyde 3-phosphate dehydrogenase (GAPDH) were purchased from Santa Cruz Biotechnology. The antibodies against iNOS and MR were purchased from Santa Cruz Biotechnology and Abcam. The antibody against arginase 1 was obtained from Sigma-Aldrich. The antibodies against F4/80 were purchased from Biolegend and AbD Serotec. The antibodies against MC1R were acquired from Alomone Lab and Santa Cruz Biotechnology. The antibodies against NF $\kappa$ B p65, phospho-NF $\kappa$ B p65 and  $\beta$ -tubulin were acquired from Cell Signaling Technology.

### **Supplementary References:**

1. Xie C, Liu K, Fu Y, *et al.* RANTES deficiency attenuates autoantibody-induced glomerulonephritis. *Journal of clinical immunology* 2011; **31**: 128-135.
2. Hayes K, Warner E, Bollinger C, *et al.* Repository corticotropin injection versus corticosteroids for protection against renal damage in a focal segmental glomerulosclerosis rodent model. *BMC Nephrol* 2020; **21**: 226.
3. Botte DA, Noronha IL, Malheiros DM, *et al.* Alpha-melanocyte stimulating hormone ameliorates disease activity in an induced murine lupus-like model. *Clinical and experimental immunology* 2014; **177**: 381-390.
4. Xie C, Sharma R, Wang H, *et al.* Strain Distribution Pattern of Susceptibility to Immune-Mediated Nephritis. *The Journal of Immunology* 2004; **172**: 5047-5055.
5. Paust HJ, Ostmann A, Erhardt A, *et al.* Regulatory T cells control the Th1 immune response in murine crescentic glomerulonephritis. *Kidney international* 2011; **80**: 154-164.
6. Arazi A, Rao DA, Berthier CC, *et al.* The immune cell landscape in kidneys of patients with lupus nephritis. *Nature Immunology* 2019; **20**: 902-914.
7. Toro-Domínguez D, Martorell-Marugán J, Goldman D, *et al.* Stratification of Systemic Lupus Erythematosus Patients Into Three Groups of Disease Activity Progression According to Longitudinal Gene Expression. *Arthritis & rheumatology (Hoboken, NJ)* 2018; **70**: 2025-2035.
8. Fang Y, Chen B, Liu Z, *et al.* Age-related GSK3 $\beta$  overexpression drives podocyte senescence and glomerular aging. *The Journal of clinical investigation* 2022; **132**.

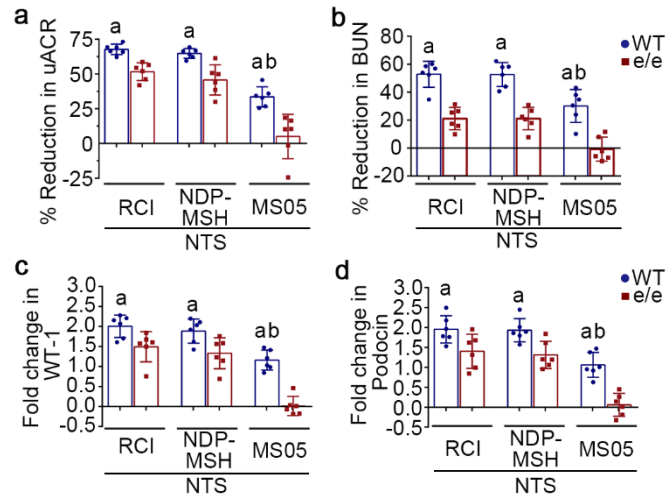


**Figure S1. The protective efficacy of melanocortin therapy against nephrotoxic serum (NTS) nephritis and related podocyte injury is blunted in *e/e* mice with melanocortin 1 receptor (MC1R) deficiency.** (a-b) Mice were treated as elaborated in Figure 1. Percentages of reduction in (a) urinary albumin to creatinine ratio (uACR) and (b) blood urea nitrogen (BUN) levels in NTS-injured mice after RCI, NDP-MSH or MS05 treatment versus vehicle treatment. (c-d) Fold changes in glomerular expression of (c) WT-1 and (d) podocin in NTS-injured mice after RCI, NDP-MSH or MS05 treatment versus vehicle treatment were calculated based on data presented in Figure 2c~2d. <sup>a</sup> $P < 0.05$  versus *e/e* mice with the same treatment; <sup>b</sup> $P < 0.05$  versus RCI or NDP-MSH treatment in WT mice with NTS nephritis; (n=6).

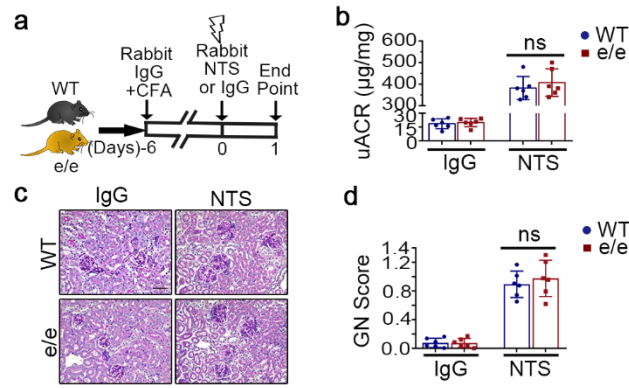


**Figure S2. WT and e/e mice exhibit albuminuria and glomerulopathy to a comparable extent in the early phase of nephrotoxic serum (NTS) nephritis.** (a) Schematic diagram depicts the model of NTS nephritis in the early phase. Wild-type (WT) and e/e mice received intraperitoneal injection of rabbit IgG emulsified in complete Freund's adjuvant 6 days before tail vein injection of rabbit NTS or nonimmune IgG. Mice were euthanized on day 1. (b) Proteinuria was estimated by urinary albumin to creatinine ratios (uACR). (c) Representative micrographs of PAS staining of mouse kidneys illustrate pathologic changes to a similar degree in WT and e/e mice, marked by mild hypercellularity of the glomeruli with segmental necrosis (Scale bar=50  $\mu\text{m}$ ). (d) Semi-quantitative morphometric analysis of glomerulonephritis (GN) score based on PAS staining of mouse kidneys. ns: not significant (n=6).

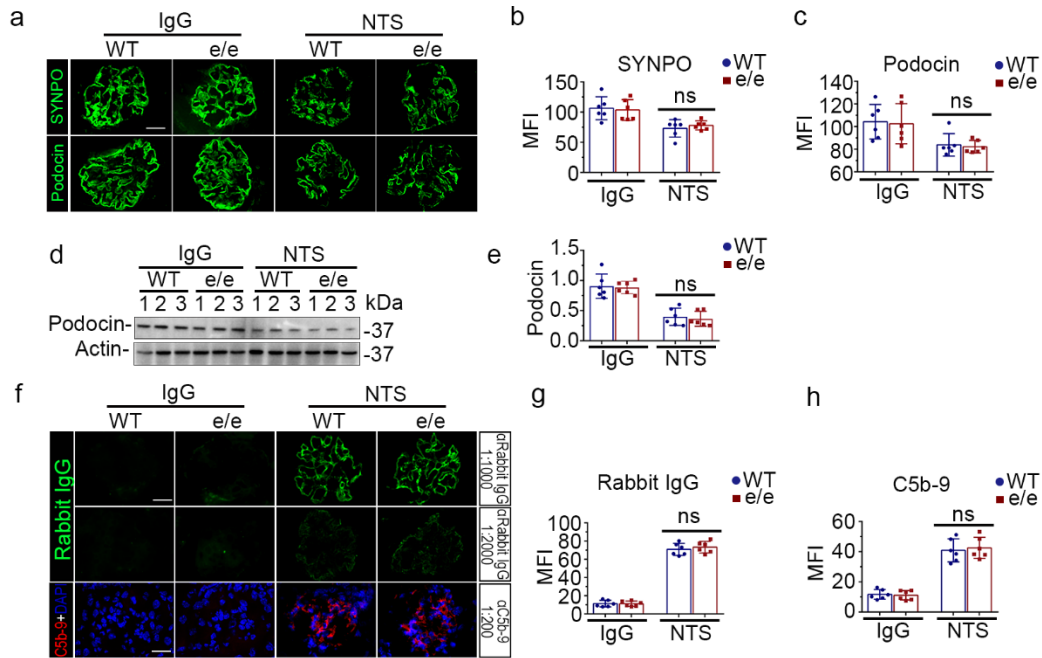


**Figure S3. Similar severity of podocyte injury is observed in WT and e/e mice in the early phase of nephrotoxic serum (NTS) nephritis.** (a) Mice were treated as elaborated in Supplementary Figure S2. Cryosections of kidney tissues were processed for immunofluorescence staining for synaptopodin (SYNPO) and podocin. Representative fluorescent micrographs are shown (Scale bar=20  $\mu$ m). (b&c) Computerized morphometric analysis of mean fluorescence intensity (MFI) of (b) SYNPO and (c) podocin staining in glomeruli. (d) Representative immunoblots showing immunoblot analysis of isolated glomeruli for podocin as well as actin, which served as a loading control. (e) Estimation of the abundance of podocin in glomeruli by densitometric analyses of immunoblots, expressed as relative levels normalized to actin levels. (f) Cryosections of kidney tissues were processed for immunofluorescence staining for rabbit IgG or C5b-9 with specific antibodies at indicated titers. Representative fluorescent micrographs are shown (Scale bar=20  $\mu$ m). (g) Computerized morphometric analysis of MFI of rabbit IgG staining (1:1,000) in glomeruli. (h) Computerized morphometric analysis of MFI for C5b-9 staining (1:200) in glomeruli. ns: not significant (n=6).

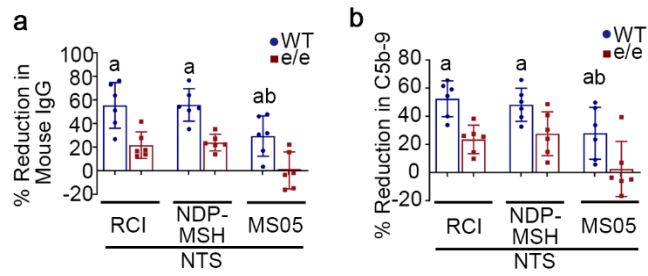


**Figure S4. The protective efficacy of melanocortin therapy against glomerular deposition of mouse IgG and C5b-9 in nephrotoxic serum (NTS) nephritis is diminished in e/e mice with melanocortin 1 receptor (MC1R) deficiency.** (a-b) Percentages of reduction in glomerular deposition of (a) mouse IgG and (b) C5b-9 in mice with NTS nephritis after RCI, NDP-MSH or MS05 treatment versus vehicle treatment were calculated based on data presented in Figure 3b-c. <sup>a</sup> $P < 0.05$  versus e/e mice with the same treatment; <sup>b</sup> $P < 0.05$  versus RCI or NDP-MSH treatment in WT mice with NTS nephritis (n=6).



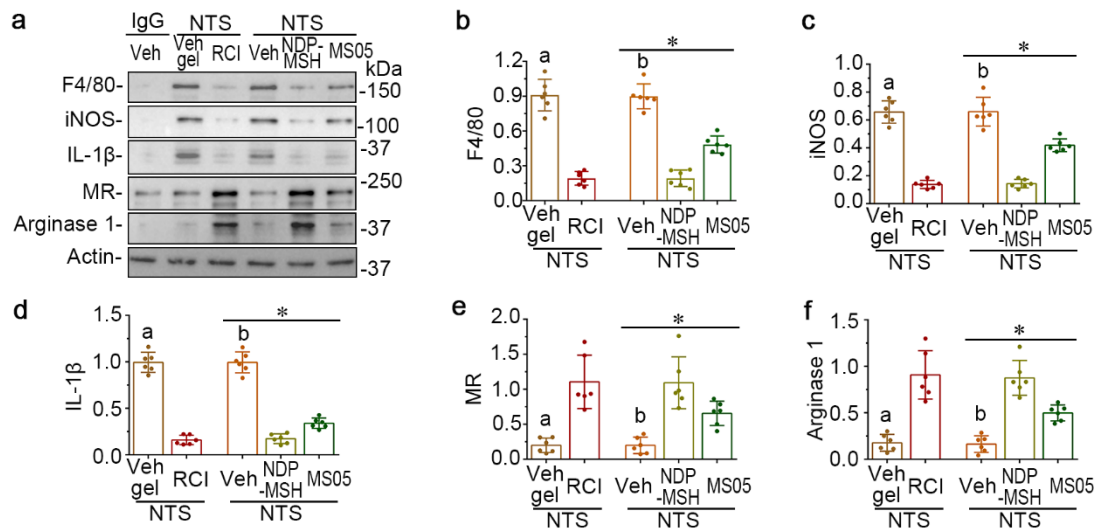


**Figure S5. Melanocortin therapy mitigates macrophage infiltration in nephrotoxic serum (NTS) nephritis, associated with an M2-skewed macrophage polarization.** (a) WT mice were injured with NTS and then treated with diverse melanocortins, vehicle (Veh) gel or Veh as elaborated in Figure 1. Representative immunoblots show the expression of various macrophage markers in the kidney. (b-f) Estimation of the abundance of (b) F4/80, (c) iNOS, (d) IL-1 $\beta$ , (e) MR and (f) arginase 1 by densitometric analyses of immunoblots, expressed as relative levels normalized to actin. <sup>a</sup> $P < 0.05$  versus NTS-injured mice treated with RCI by unpaired  $t$  test; \* $P < 0.05$  by ANOVA; <sup>b</sup> $P < 0.05$  versus NTS-injured mice treated with NDP-MSH or MS05 (n=6).

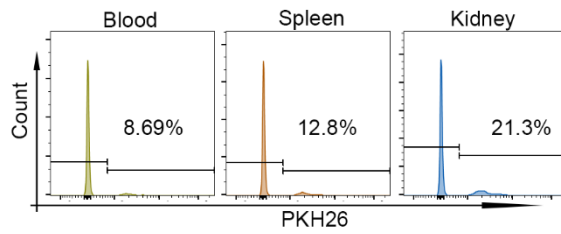


**Figure S6. Red fluorescent dye PKH26<sup>+</sup> donor chimerism is achieved in the blood, the spleen and the kidney of recipient mice with nephrotoxic serum (NTS) nephritis.** WT mice received adoptive transfer of WT BMDC and then developed NTS nephritis as elaborated in Figure 7. Peripheral blood mononuclear cells, splenocytes and kidney leukocytes were prepared (pool of 3 animals per group). Flow cytometry plots show percentage of PKH26<sup>+</sup> cells among CD45<sup>+</sup> hematopoietic cells prepared from the blood, spleen and kidney of recipient mice.

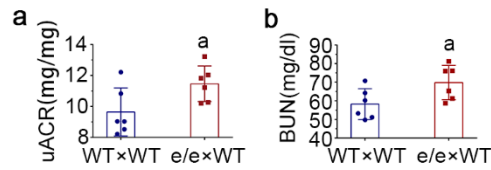


**Figure S7. Adoptive transfer of bone marrow-derived cells (BMDCs) prepared from syngeneic e/e mice worsens proteinuria and kidney dysfunction in WT mice with nephrotoxic serum (NTS) nephritis.** WT recipient mice received adoptive transfer of WT or e/e BMDC and then developed NTS nephritis as depicted in Figure 7a. (a) Proteinuria was estimated by urinary albumin to creatinine ratios (uACR). (b) Kidney function was assessed by measuring blood urea nitrogen (BUN) levels in sera. <sup>a</sup> $P < 0.05$  versus WTxWT group (n=6).

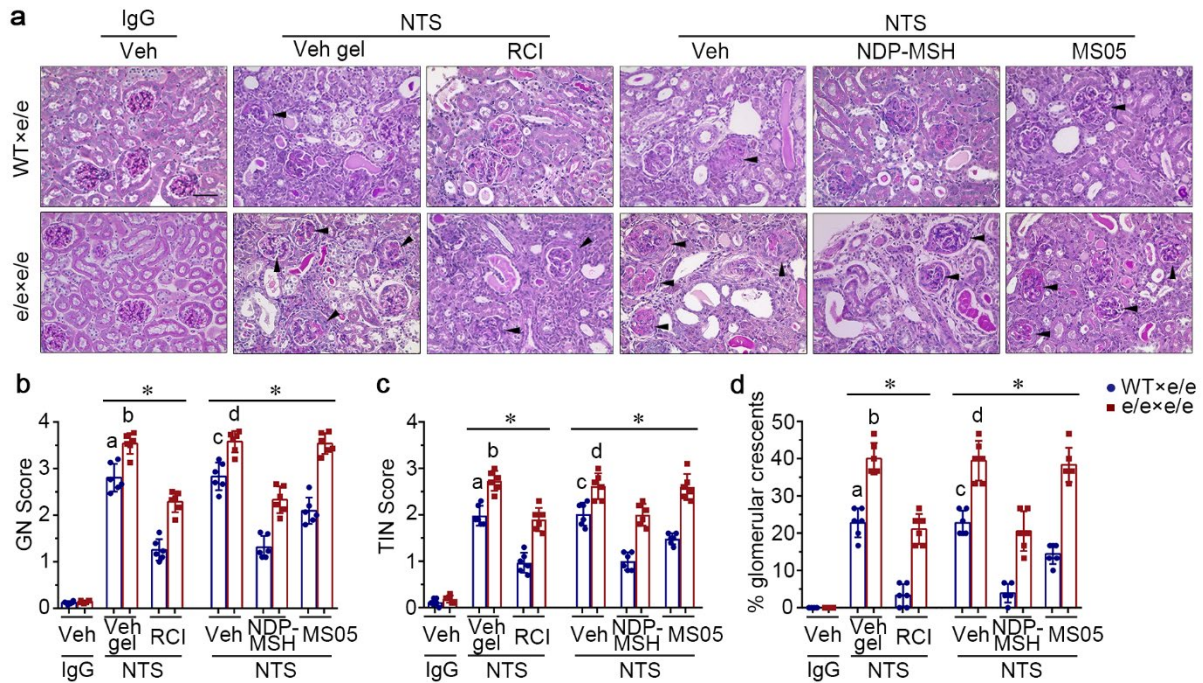


**Figure S8. Adoptive transfer of bone marrow-derived cells (BMDCs) prepared from syngeneic WT mice alleviates kidney injury and dysfunction in e/e mice with nephrotoxic serum (NTS) nephritis, and reinstates the protective efficacy of melanocortin therapy.** Mice were treated as described in Figure 7. (a) Representative micrographs show periodic acid-Schiff (PAS) staining of kidney specimens. Arrowheads indicate glomeruli with crescents (Scale bar = 50  $\mu$ m). (b–d) Semi-quantitative morphometric analysis of (b) glomerulonephritis (GN) score, (c) tubulointerstitial nephritis (TIN) score, and (d) the percentage of glomeruli having crescents based on PAS staining of mouse kidneys. \* $P < 0.05$  by ANOVA; <sup>a</sup> $P < 0.05$  versus NTS-injured mice treated with e/e BMDC and Vehicle gel (Veh gel) or with WT BMDC and RCI; <sup>b</sup> $P < 0.05$  versus NTS-injured mice treated with e/e BMDC and RCI; <sup>c</sup> $P < 0.05$  versus NTS-injured mice treated with e/e BMDC and Vehicle (Veh) or with WT BMDC and NDP-MSH or MS05; <sup>d</sup> $P < 0.05$  versus NTS-injured mice treated with e/e BMDC and NDP-MSH; (n=6).

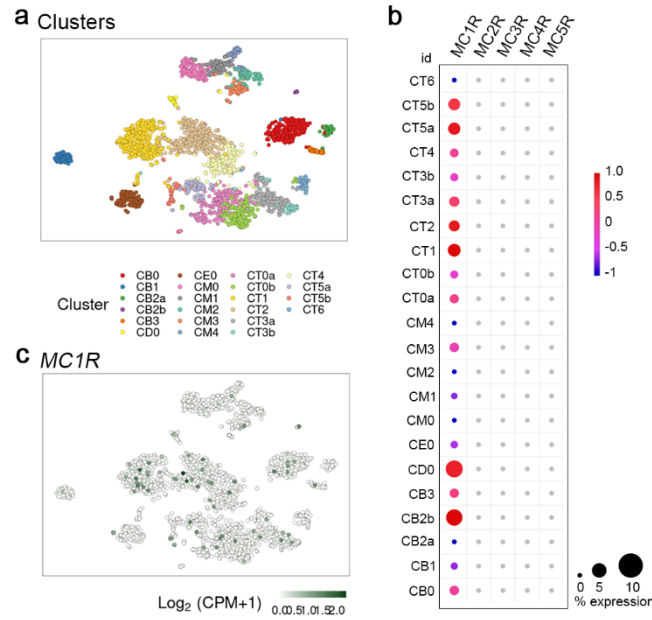


**Figure S9. Melanocortin 1 receptor (MC1R) is expressed by diverse kidney leukocyte subsets based on single cell RNA sequencing analysis of kidney biopsies from lupus patients.** A *post hoc* analysis of single cell RNA sequencing (scRNAseq) transcriptome of kidney leukocytes in kidney biopsies from lupus patients based on the Accelerating Medicines Partnership (AMP) phase I studies of lupus nephritis was performed to evaluate the mRNA expression of various MCRs in kidney leukocyte subsets. (a) T-distributed stochastic neighbor embedding (t-SNE) plot illustrates kidney immune cells in human kidneys with lupus nephritis. Different colors indicate clusters identified by unsupervised clustering analysis. (b) Dot plot showing gene expression levels of *MC1R*, *MC2R*, *MC3R*, *MC4R*, and *MC5R* in diverse kidney leukocyte clusters. (c) Feature plot showing *MC1R* expression in different kidney leukocyte clusters. Figures were generated using the viewing browser <https://immunogenomics.io/ampsle/> or [https://singlecell.broadinstitute.org/single\\_cell/study/SCP279/amp-phase-1](https://singlecell.broadinstitute.org/single_cell/study/SCP279/amp-phase-1). CM0, Inflammatory CD16<sup>+</sup> macrophages; CM1: Phagocytic CD16<sup>+</sup> macrophages; CM2, Tissue-resident macrophages; CM3, Conventional dendritic cells; CM4, M2-like CD16<sup>+</sup> macrophages; CT0a, Effector memory CD4<sup>+</sup> T cells; CT0b, Central memory CD4<sup>+</sup> T cells; CT1, CD56dim CD16<sup>+</sup> NK cells; CT2, Cytotoxic T lymphocytes; CT3a, Tregs; CT3b, TFH-like cells; CT4, GZMK<sup>+</sup> CD8<sup>+</sup> T cells; CT5a, Resident memory CD8<sup>+</sup> T cells; CT5b, CD56 bright CD16<sup>-</sup> NK cells; CT6, ISG-high CD4<sup>+</sup> T cells; CB0: Activated B cells; CB1, Plasma cells/Plasmablasts; CB2a, Naive B cells; CB2b, Plasmacytoid dendritic cells; CB3, ISG-high B cells; CD0, Dividing cells; CE0, Epithelial cells.

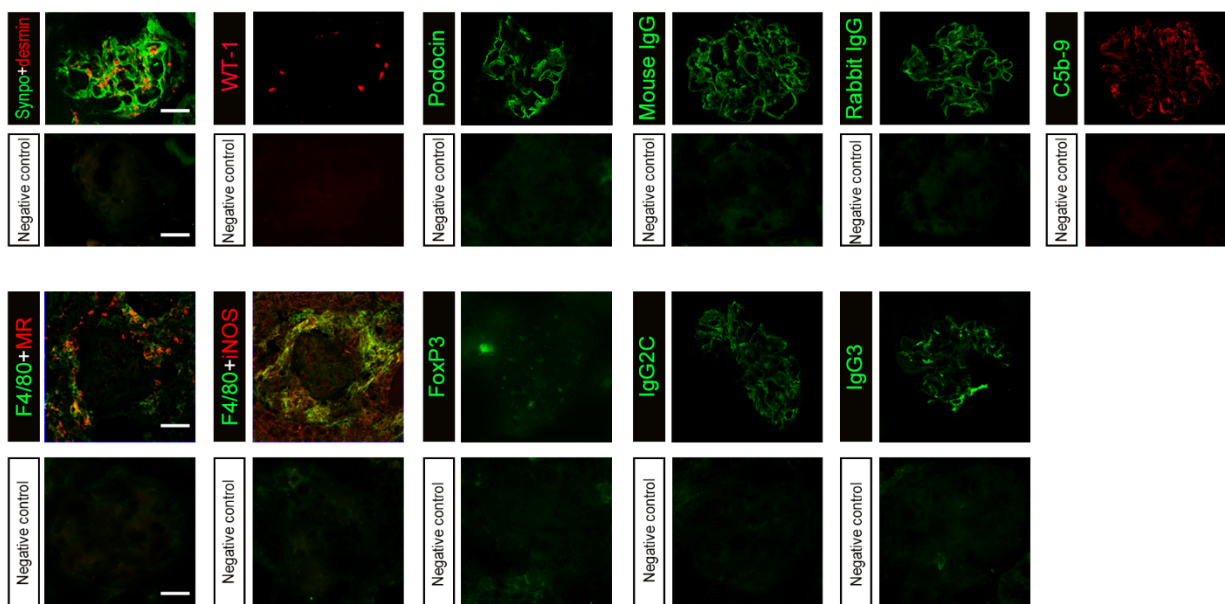


**Figure S10. Negative controls for immunostainings.** Cryosections of mouse kidneys were processed for fluorescent immunohistochemistry staining for indicated proteins by using specific primary antibodies, followed by staining with Alexa Fluor-conjugated secondary antibodies as needed. As negative controls, the primary antibodies were replaced by IgG isotype controls from the same species of the primary antibodies and no specific staining was noted. Alternatively, as negative controls for staining heterologous or autologous IgG, Alexa Fluor-conjugated anti-goat IgG instead of Alexa Fluor-conjugated anti-rabbit or anti-mouse IgG was applied and no specific staining was detected. (Scale bar = 20  $\mu$ m).